POLITECNICO DI TORINO
Repository ISTITUZIONALE

Realistic air filter media performance simulation. Part II: Beyond finite-volume computational fluid dynamics procedures

(Article begins on next page)

28 April 2024

Realistic Air Filter Media Performance Simulation: Part II: Beyond Finite-Volume CFD Procedures

Bin Zhou PhD [a] , Paolo Tronville PhD [b] & Richard Rivers [c]

[a] College of Urban Construction and Safety Engineering, Nanjing University of Technology, Nanjing, China

[b] Department of Energy - Politecnico di Torino, Corso Duca degli Abruzzi 24, I-10129, Turin, Italy

[c] EQS Inc., Louisville, Kentucky, U.S.A.
Accepted author version posted online: 20 Feb 2013.

PLEASE SCROLL DOWN FOR ARTICLE

Realistic Air Filter Media Performance Simulation:

Part II: Beyond Finite-Volume CFD Procedures

Author:

Bin Zhou (PhD)

College of Urban Construction and Safety Engineering,

Nanjing University of Technology

Nanjing, China

E-mail: zhoubinwx@hotmail.com

Corresponding Author:

Paolo Tronville (PhD, ASHRAE Member)

Department of Energy - Politecnico di Torino

Corso Duca degli Abruzzi 24

I-10129 Turin

Italy

Telephone: +39 011 0904477

Fax: +39 011 0904499

E-mail: paolo.tronville@polito.it

Author:

Richard Rivers (ASHRAE Fellow)

EQS Inc., Louisville, Kentucky U.S.A.

E-mail: rdrivers@bellsouth.net

One form of numerical simulation of flow and particle capture by air filter media sees gases as continuous fluids, influenced by the macro properties viscosity, density and pressure. The alternate approach treats gases as atoms or molecules in random motion, impacting their own kind and solid surfaces on a micro scale. The appropriate form for analysis of flow through given filter medium at a given operating condition depends on the gas condition and the Knudsen number (Kn) of the finest fibers in the filter medium simulated. Continuum, macro-scale methods may be usable for media with individual fiber Kn as high as 0.01. In Part I of this paper, we discussed simulations of air filter media performance where all fibers are in the continuum flow regime, and the Navier-Stokes equation with finite-volume solution is applicable. Here, in Part II, we discuss filter media performance simulation by computational approaches other than numerical solutions of the Navier-Stokes equation. These include use of the Burnett, Super Burnett and Grad Moment equations; Lattice-Boltzmann and Direct Simulation Monte Carlo methods; and the Molecular Dynamics, Boundary Singularity and Boundary Element methods.

INTRODUCTION

Part I of this paper discussed restrictions in using computational fluid dynamics (CFD) to simulate fibrous air filter media performance. Filters may operate at altitudes where air can no longer be considered a continuous fluid. The diameters of fibers used in filter media are also often small enough that thermodynamic equilibrium is not maintained at fiber boundaries. Simulations of gas flow cannot then use the Navier-Stokes equation reliably. The criterion for changes in flow regime is the Knudsen number, *Kn*, equal to the mean free path of the flowing

gas divided by a characteristic measure of fiber size. For the usual fibers having circular cross sections, the measure is the fiber diameter; for other shapes, the hydraulic diameter may serve.

For flow geometries with *Kn* between about 0.01 and 1.0, partial differential equations other than the Navier-Stokes equation exist that do describe the flow reliably, and numerical solution techniques have been developed to solve these equations. These equations include the Burnett, "Super Burnett" and Grad Moment equations.

Fundamentally different methods have been developed to simulate situations where *Kn* is greater than 0.01. Two methods, Lattice-Boltzmann (LB) and Direct Simulation Monte Carlo (DSMC), mimic the behavior of single gas molecules by tracking packets of molecules from collision to collision through the simulated geometry, based on defined velocity distributions of the molecules and momentum exchange rules. DSMC and LB are computationally robust, and usable for all flow regimes except when *Kn* values greater than 1.0 exist. This value of *Kn* approximates the lower limit of free-molecular flow, when gas molecule impacts with solid boundaries are rare. For this regime, the Molecular Dynamics (MD) method has been developed. It simulates the tracks of single molecules through a flow geometry, avoiding assumptions about molecular velocity distributions.

Still other methods, the Boundary Singularity Method (BSM) and the Boundary Element Method (BEM) exist. BSM uses "stokeslets", potentials defined relative to a specified point either on or near boundaries. These potentials each provide solutions to Stokes' equation throughout the domain. The strengths of the stokeslets are adjusted so that the sums of their

solutions at all discretized boundary points match the boundary conditions with some chosen accuracy. BSM appears to be limited to geometries simpler than air filter media.

BEM avoids discretization of the entire computational domain. Discretization is required only along the domain outer boundaries and the boundaries of the bodies within the domain (fibers in the case of filter media simulation). At these boundaries, the velocity relationships are expressed in terms of *integral* solutions to the governing gas-flow partial-differential equations. Such solutions exist for the case of the Navier-Stokes equation and circles, and BEM may allow faster calculations of filter media simulation in the continuum and transitional regimes. Semi-empirical methods, e.g. one which treats filter media as formed of microscale pores, have also been developed. We describe each method briefly, and evaluate their ability to predict the performance of fibrous filter media based on actual media geometries.

DSMC and LB have become reference methods for validation of other CFD computational methods, by comparison runs with identical geometries, and identical gas conditions. Table 1 shows the approximate *Kn*-defined limits to the several flow regimes, and the computational methods usable in each sub-regime. This table modifies the one appearing in Yun and Agarwal (2002) to include BEM, BSM and MD, and to reflect what we believe to be more reliable Kn limits for some regimes obtained from our literature survey. Gad-el-Hak (1999) is an informative introduction to the analysis of flow in micro- and nano-scale geometries.

SIMPLIFYING ASSUMPTIONS

Part I examined the range of fiber diameters and operating conditions for air filter media, and justified some simplifying assumptions:

ACCEPTED MANUSCRIPT

- Reynolds numbers of fibers in air filter media are always low enough that there is no turbulence inside the filter media.

- Filter media flow is "incompressible", too low for shock to occur. Gas thermophysical properties can be assumed constant in a single simulation.

- We can ignore the effects of gravity, convection, centrifugal force or any other external forces on the gas flows.

- Electrostatic effects are important to fibrous media filtration. However, we limit discussion to charge-free fibers and "neutral" aerosols, which in fact carry charges according to the Boltzmann distribution. Electrostatic image forces should therefore be included in simulations.

Throughout both papers, $Kn = \lambda/d$, where λ is the mean free path of the molecules of the flowing gas, and d is the diameter of the fiber or particle. Many studies have defined Kn in terms of radii, which gives Kn values twice as large as our definition.

MOMENTUM EXCHANGE

Molecular Interaction in Gases

Analysis of the flow through geometries of all scales begins with the momentum exchange between a single pair or group of molecules. Figure 1 plots the potential energy of interaction between a pair of molecules as a function of the distance r between their centers. This potential defines the forces of attraction and repulsion between the two colliding molecules. The figure shows three approximations to the actual potential. At a distance, the energy interaction

ACCEPTED MANUSCRIPT

and hence force is negligible, but a force of attraction increases to the maximum value E as r decreases. The attractive force then declines as the molecules come closer together; at separation r_{LJ}, the molecules "collide"; the force between them changes to repulsive, and they can approach no closer to each other. The molecules exchange some or all of their momenta, and change paths. For the rigid (hard) sphere model there is no attractive force. The square-well potential model has both attraction and repulsion, but is a rough, discontinuous approximation to the actual potential. The Lennard-Jones potential is continuous, and creates both attraction and repulsion, hence is closer to reality.

Boltzmann Equation

In the 19th century, Clausius, Euler, Maxwell, Boltzmann, and others developed the principals of thermodynamics from molecular collision models. Molecules have a velocity distribution f at every time t and position r in the space occupied. This leads, with some simplification, to Boltzmann's transport equation.

In the Boltzmann concept, two spaces are defined: the first, a "position space", the usual 3D space where the position of the molecules is specified by three coordinates (e.g. x_1, x_2, x_3). The second space is a "velocity space", in which each point denotes a set of three components of the vector velocity **v**, i.e. (v_1, v_2, v_3). The distribution of molecular velocities in the position space changes with time t, and is given by the function $f(v_i, x_i, t)$ for the class of molecules whose behavior the equation describes, and by $f_c(v_i, x_i, t)$ for the class of molecules with which it collides.

ACCEPTED MANUSCRIPT

One form of the Boltzmann equation, for a simple dilute gas, is:

$$\frac{\partial}{\partial t}(nf) + \mathbf{v} \bullet \frac{\partial}{\partial x_i}(nf) + \mathbf{F} \bullet \frac{\partial}{\partial \mathbf{v}}(nf) = \int\limits_{-\infty}^{\infty} \int\limits_{0}^{4\pi} n^2 (f^* f_c^* - f^* f_c^{'}) v_r s \cdot d\theta_s \cdot d\mathbf{v}_1 \qquad (1)$$

Where

$\mathbf{F}$ represents all the external forces per unit mass of the molecule (e.g. gravity), assumed constant in the velocity space;

n is the number of molecules per unit volume;

f is $f(v_i, x_i, t)$, the velocity distribution functions at time t;

The right-hand term is the "collision integral", where

f^* is the distribution of velocities of the described molecules after the collision;

f_c^* is the distribution of velocities of the colliding molecule after the collision;

s is the collision cross-section for the molecule;

θ_s is the solid angle about the collision point;

v_r is the ratio of the absolute values of the velocities of the two molecular classes at time t, i.e. $|v//|v_c|$.

Solving the Boltzmann equation numerically in the way in which the Navier-Stokes, Burnett, and Grad moment equations are solved is demanding computationally, and in some cases, not possible. Instead, the Lattice-Boltzmann method and other schemes are used, as

7

described below. We include this discussion of the Boltzmann equation because it can be the starting point for derivation of most governing equations, and is referenced often in discussions of flows in micro-scale geometries. Such derivations involve pages of mathematics, and are full of caveats about singularities and the stability and computational complexity of the resulting governing equation sets.

The interaction of gas molecules with surfaces and definitions of slip, slip coefficient, accommodation coefficient, and the influence of these factors on flow around small cylinders and spheres are discussed in Part I of this paper. Here our concern will be with the right-hand side of Equation 2, the collision integral, for which various approximations produce the Burnett, Super-Burnett, and Grad Equations. These either cannot be solved by the same procedures used to solve the Navier-Stokes equations, or are more effectively solved by other means. Finally, we discuss procedures used for solutions in the free-molecular regime.

GOVERNING EQUATIONS AND COMPUTATION METHODS

One transformation of Equation 1 produces the well-known Navier-Stokes momentum equation. For those combinations of fibrous filter media diameters and gas conditions that produce fiber Kn values below 0.001, the Navier-Stokes momentum equation with proper boundary conditions and equation solvers can yield reliable simulations. For $0.001 < Kn < 0.01$, the results are less certain, but sometimes acceptable, without resorting to other computational methods. Hadjiconstantinou (2006) discusses the limits of Navier-Stokes applicability. Verification of CFD-calculated values against measured pressure drops is essential when Kn values > 0.001 exist.

Commercial CFD codes do not necessarily include the alternate procedures LB, DSMC, MD, BEM and BSM. Academic and open-source CFD packages often do provide these methods. Internet sites www.openfoam.com and www.cfd-online.com provide entries related to these techniques as well as finite-volume CFD. Extensive literature on parallel-computing techniques is provided by manufacturers of graphic processing units (GPUs) which allow parallel-computing on desktop computers.

Burnett and Super-Burnett Equations

Several sets of Burnett equations are used to describe micro- and rarefied-gas flows. The equations have been developed to allow the solution of partial differential equations to be used for regimes where NS cannot be used and LB and DSMC have high computational burdens. However, many problems have arisen in the use of Burnett equations, instabilities and even violation of the laws of thermodynamics. Bobylev (2006), Struchtrup (2005), Söderholm (2007), and Struchtrup and Taheri (2011) discuss these problems.

The basic difference between the various forms of the Burnett and Super-Burnett equations is in the definition of the collision integral, the right-hand side of Equation 1. There are many textbooks and journal articles treating the various forms in detail, among them Chapman and Cowling (1970); Bird (1994); Cercignani (2000); Agarwal et al. (2001); and Karniadakis et al. (2005). Struchtrup and Taheri (2011) provide an introduction to the method. Use of the Burnett equations requires a full understanding of the mathematics and physics involved. They do not appear to be convenient for the wide range of flow regimes met in simulations of fibrous air filter performance.

Grad Moment Equations

In its simplest form, for a monatomic ideal gas, the Boltzmann equation becomes:

$$\frac{\partial}{\partial t}(nf) + \mathbf{v} \bullet \frac{\partial}{\partial x_i}(nf) = St(nf) \tag{2}$$

where $St(nf)$ is the "collision term", defining the change in the molecular velocity distribution function f which occurs at a molecular collision. The complete Navier-Stokes equations defining fluid flow have five macro variables at each point in the fluid-filled space: density, velocity, temperature, heat flux and stress tensor (which gives rise to viscosity). These macro variables can be obtained by integration of five micro variables of the velocity distribution of the gas molecules at the point in question. These micro variables are mass density ρ; temperature T; heat flux components $q_i = (q_1, q_2, q_3)$; flow velocity components $v_i = (v_1, v_2, v_3)$; thermal velocity V_T; and stress tensor components $\sigma_{ij} = (\sigma_{11}, \sigma_{12}, \sigma_{23}, \sigma_{22}, \sigma_{33})$.

The 13 variables are the "moments" of the distribution function f which appear in the much-investigated 13-moment method developed by Grad (1949) to extend hydrodynamic solutions to about Kn=0.5. His equations for 16 moments are shown here in Equations 6 and 7. Grad reduced the number of moments to 13 by setting $m_{ijk} = R_{ik} = \Delta = 0$. He later added other moments, producing his 26-moment method, which is usually reliable to about $Kn = 1.0$. Mass, momentum and energy in the system must be preserved, so Grad had:

$$\text{(mass)} \qquad \frac{\partial \rho}{\partial t} + \frac{\partial \rho v_k}{\partial x_k} = 0 \tag{3}$$

$$\text{(momentum)} \qquad \frac{\partial \rho v_i}{\partial t} + \frac{\partial}{\partial x_k}(\rho v_i v_k + P\delta_{ik} + \sigma_{ik}) = 0 \tag{4}$$

10

(energy) $\quad \dfrac{\partial}{\partial t}(\rho\varepsilon + \tfrac{1}{2}\rho v_i^2) + \dfrac{\partial}{\partial x_k}(\rho\varepsilon v_k + \tfrac{1}{2}\rho v_i^2 v_k + Pv_k\delta_{ik} + \sigma_{ik}v_i + q_k) = 0$ $\qquad$ (5)

In Equation 5, $\varepsilon = kT/m$, where k is the Boltzmann constant, 1.3806448 x 10^{-3} J/K, and m is the mass of an atom; hence ε is simply a different unit for temperature. δ_{ik} is Kronecker's delta, = 0 if j $\neq$ k, = 1 if j=k.

An equation was needed for the stress deviator:

$$\frac{\partial \sigma_{ij}}{\partial t} + \frac{\partial \sigma_{ij}v_k}{\partial x_k} + \frac{4}{5}\frac{\partial q_{\langle i}}{\partial x_{j\rangle}} + 2\sigma_{k\langle i}\frac{\partial v_{j\rangle}}{\partial x_k} + \frac{\partial m_{ijk}}{\partial x_k} + 2P\frac{\partial v_{\langle i}}{\partial x_{j\rangle}} = -\frac{P}{\mu}\sigma_{ij} \qquad (6)$$

and for the heat flux:

$$\frac{\partial q_i}{\partial t} + \frac{\partial q_i v_k}{\partial x_k} + \frac{5}{2}\sigma_{ik}R\frac{\partial T}{\partial x_k} + RT\frac{\partial \sigma_{ik}}{\partial x_k} - \sigma_{ik}RT\frac{\partial \ln\rho}{\partial x_k} - \frac{\sigma_{ij}}{\rho}\frac{\partial \sigma_{jk}}{\partial x_k} + \frac{7}{5}q_k\frac{\partial v_i}{\partial x_k}$$

$$+\frac{7}{5}q_i\frac{\partial v_k}{\partial x_i} + \frac{2}{5}q_i\frac{\partial v_k}{\partial x_k} + \frac{1}{2}\frac{\partial R_{ik}}{\partial x_k} + \frac{1}{6}\frac{\partial \Delta}{\partial x_i} + m_{ijk}\frac{\partial v_j}{\partial x_k} + \frac{5}{2}PR\frac{\partial T}{\partial x_i} = -\frac{2P}{3\mu}q_i \qquad (7)$$

Indices marked $i\rangle$ or $\langle i$ denote symmetric trace-free parts of tensors. These terms were added by Grad to the Navier-Stokes-Fourier equations to stabilize their solutions and provide reliable descriptions of shock, Knudsen layers, and the phenomena of rarefied gas and microscale aerodynamics. Torrilhon and Struchtrup (2008) review methods improving on Grad's concept. In spite of the complexity introduced by adding moments, the increase in range of *Kn* values for reliable simulations using Grad's methods has been limited, and there are subtle traps in their use. Computing power has also increased, making LB and DSMC procedures more practical, hence the shorter computation times obtained with Grad's methods are less important. LB and DSMC are preferred for simulations with 0.1 < *Kn* < 10, and MD required for *Kn* > 10.

Lattice-Boltzmann Method

For simplicity, we limit our description of LB to the two-dimension (2D) case. Analogous patterns exist for 3D simulations. LB in a limited way models the behavior of individual molecules, substituting packets of "computational molecules" many million times more massive than an actual single molecule of the gas. Changes in the position and velocity of molecular packets are assumed to occur at discrete time steps rather than continuously, as is the case with differential equations. An array of nodes, a "lattice", is constructed, covering the simulation domain. Nodes are equally spaced from each other, but the overall domain can be divided into zones with different lattice scales. Figure 2 shows a square array, with columns and rows of nodes equally-spaced by distance L_2; other patterns are possible. The figure shows lattice with nodes added along a curved boundary. This avoids the jagged approximation to boundary shapes which occur with any uniformly-spaced lattice. Interpolation for additional values along function-defined boundaries is not difficult, because of the simpler geometry of a regular lattice.

At each node of the lattice there are distribution functions f_1, f_2, f_3, ..., f_n, expressing the number of identical molecules at that point having n discrete vector velocities $\mathbf{v}_1$, $\mathbf{v}_2$, $\mathbf{v}_3$, ..., $\mathbf{v}_n$. For a 2D lattice (Figure 3) $n = 9$, with 8 vectors pointing to a nearest neighbor point, and a zero vector at the node. The vector sum of the nine gives the mean velocity of the molecules associated with the point, which corresponds to the velocity of the fluid located at that point at time t. At each time step, the molecular packets collide, and the velocities are redistributed between the packets leaving each point. Collision rules must be chosen to define the exchanges in a collision, and to conserve the total number of molecules, the total momentum, and total energy of the packet. In Figure 3A, summing the vectors at the node shows the packet of

molecules at rest. In Figure 3B, at a later time t_2, the packet is moving approximately in the direction of vector $\mathbf{v}_5$. (Note: the order in which the vectors are numbered is immaterial, provided it is consistent throughout a defined section of the domain)

Succi (2001), Wagner (2008) and Luo, Krafczyk, and Shyy (2010) provide detailed discussions of the LB method. Introductions by Chen, Doolen and Eggert (1994) and Succi et al (2010) are also available on the Internet. The review by Mei, Shyy, Yu and Luo (2002) of LB as it applies to curved boundaries is directly concerned with the problems met in filter media simulation.

Direct Simulation Monte-Carlo Method

DSMC begins with the principles on which the Boltzmann equation is built. Like LB, it simulates actual molecules with packets containing large numbers of individual molecules, typically $> 10^{12}$ for 3-D simulations. DSMC defines a grid of equally-dimensioned cells covering the computational domain. In the scheme developed by Bird (1994) these cells are divided into equally-dimensioned sub-cells. For accurate results, the smaller cells must have sides far shorter than the gas mean free path. Molecular packets selected randomly move in finite time steps from sub-cell to sub-cell. The position of each packet after a time step is determined by its velocity, and no collisions are assumed to occur until the packet reaches its destination sub-cell. The velocities of the packets are distributed in cells at the start of the calculation according to a function appropriate to the gas temperature and other conditions, with assignments made by a random-number generator. The initial directions are also determined by random numbers, with all directions equally probable. At the destination cell, collisions occur, with results dependent on the velocities and directions of both molecular packets colliding, and interaction rules chosen by

13

the user. Some of the sub-cells will lie on boundaries, where different collision interactions are defined.

Macro properties of the gas, such as bulk velocity in a region having a substantial number of sub-cells, are obtained by periodically averaging velocity over the sub-cells. Where thermal effects are modeled, temperature, being a function of velocity squared, is obtained by summing sub-cell velocities squared. The scheme allows much flexibility, including boundary slip, heat transfer, and chemical reactions.

Several introductions to DSMC methods are available (e.g. Macrossan (2006), which includes code). Bird, whose work established the method, updates his presentation in Bird (1994). He now maintains a site on the internet (www.gab.com.au/) with introductory material and software allowing solutions of some DSMC problems in 2- and 3-dimensions. Baker and Hadjiconstantinou (2005) and Radtke, Hadjiconstantinou, and Wagner (2009) present modifications to the DSMC method which shorten computation times and improve accuracy.

Molecular Dynamics Method

The Molecular Dynamics method (MD) tracks the behavior of single molecules, making no assumptions about the distribution of the velocities of these molecules. The computational burden for this is large, but parallel-processing techniques are advancing rapidly. The website http://lammps.sandia.gov/ offers much information, including code. A rigorous introduction by Allen (2004) is available and a visual introduction to the method can be accessed at http://www.personal.psu.edu/auk183/MolDynamics/Molecular Dynamics Simulations.html.

O'Connell and Thompson (1995) describe a hybrid computation scheme, which treats computations near boundaries separately from the gas-filled spaces between. They analyze a

very simplified geometry (Fig. 4). They establish a thin layer close to the solid boundary A where they use the MD method, and a thicker zone extending from boundary B where they use the Finite Difference Method (FDM). In their model, Boundary A is stationary, boundary B moving with a velocity that increases with time. The two zones overlap somewhat about line C. The method is designed to make the molecular velocity distributions in the overlap zone continuous. There is no experimental verification of the method, but the results of this hybrid method exactly match MD results carried out for the entire space. In our opinion, they show on theoretical grounds that for a given geometry, both the FDM and the MD method are equally accurate, provided the gas/boundary interactions are described correctly. Whether this is true for the complex geometry of filter media, and the highly curved boundaries in media, would require careful comparison between simulation and measurements made on media with a wide range of fiber diameters.

Boundary Singularity Method and Stokeslets

A "stokeslet" is a solution to Stokes' equations, representing the velocity in the surrounding space resulting from an external force acting on a single point. The Stokes' equations are:

$$\mu \diamond u = \nabla p - \mathbf{F} \tag{8}$$

$$\nabla \diamond \mathbf{u} = 0 \tag{9}$$

Where μ is absolute viscosity, p is pressure, $\mathbf{u}$ is (vector) velocity, and $\mathbf{F}$ the (vector) force. $\mathbf{F}$ is a function of distance from a single point specified by a potential field of some specified strength, originating at the point. For flow around a circular object, in two dimensions, stokeslets are

located at equal angular spacing around the circle. The velocity at any point within the flow domain is the vector sum of the contribution at that point from all the stokeslets. The strength of each stokeslet is adjusted in steps until the velocities at the domain boundaries and the velocities at the circle boundary match the boundary-condition values throughout the domain.

Zhao and Povitsky (2008, 2009) studied the cases of 2D flow around a single circle and various arrays of circles. They show that better results are obtained if the stokeslets are *submerged*, that is, located inside the circles, rather than at the circle radius. This is not unreasonable, for stokeslets are not physical entities, but merely computational devices. The paper gives procedures to determine the optimum level of submergence. It also discusses how computation time may be reduced by a hybrid technique, using BSM in the immediate vicinity of the circles representing fibers, and DSMC in the spaces between them. These methods show promise, and are worth further investigation, especially on more realistic media models than the regular arrays analyzed in many papers.

Boundary Element Method

The Boundary Element Method (BEM), sometimes called the Boundary Integral Method (BIM) or Boundary Integral Element (BIE) technique, the numerical solution deals with integrals, rather than partial differential equations. It must be possible to obtain a general integral solution to the partial differential equation describing the flow field. This is true for the Navier-Stokes equations, but only at low Mach and Reynolds numbers, which fits essentially all filter media applications. Comacho and Barbosa (2005) give a sample solution meeting these criteria. The method permits flow calculations beyond the continuum regime, to *Kn* values as great as 0.1. In BEM, boundaries are discretized - into line segments for 2D analysis, surface elements in

3D analysis – but there is no need to provide a discretizing grid in the flow spaces between boundaries.

The values of the flow equation integrals are defined at a point on each boundary element, as are the boundary conditions at that point. Calculation then proceeds with time-steps like other methods, until some chosen error in velocities at all the boundary elements is achieved. The time required for calculation is generally much smaller than for finite volume, because calculations for error are limited to the boundary elements. Accuracy is better, because the integrals are exact representations of the influence of the boundaries on the flow. Velocity vectors at any point in the flow space can be calculated by summing the effects for that point of the integral "stokeslets" on each boundary element, effects dependent only on the distance between the boundary element points and the chosen flow-field point. There is some argument over how much computational burden is reduced (Muhammad, 2009). The method should be investigated further, especially when more realistic models for filter media geometry and dust loading are tried.

Modified Navier-Stokes Methods

Sambaer, Zatloukai and Kimmer (2011) used very realistic 3D media models with random fiber diameters and locations, but assumed that gas flowed through the media in parallel lines, undisturbed by the fibers. The model can predict capture of very large and very small-particles, but fails with intermediate particle diameters where inertial effects are important. In Sambaer, Zatloukai and Kimmer (2012) these same authors simulated pressure drop and particle capture for two filter media fabricated using nanofibers. The media was modeled by pores having uniform diameter and length, values derived from SEM images of the actual fibrous

media. The diffusion of particles to the walls of the "pores" was calculated using the Navier-Stokes equation with an artificial viscosity as proposed by McNenly, Gallis and Boyd (2005). The pressure drop and particle capture calculated matched measured values well, but the relation of pore dimensions to actual media geometry may not hold for all media. These authors limit the expression for modified viscosity to (pore) *Kn* values less than 0.1, and to simple geometries such as uniform-diameter pores. The model does not appear adaptable to fibrous filter media in general, and all particle diameters.

Wang (2002) applied the "eigenfunction expansion" technique to solve the Navier-Stokes equation for several regular arrays of cylinders. It may be possible to expand this to randomized models.

SIMULATION OF AEROSOL PARTICLE CAPTURE

Particle capture by a filter medium is simulated by tracking the paths of particles through the simulated flow field in the medium. Two basic methods are available: Lagrangian and Eulerian. These methods are described in Part I of this paper. The Lagrangian method essentially traces the trajectory of particles from domain cell to cell, using Newton's second law with expressions for the forces on the particle. These forces include aerodynamic drag, Brownian impacts, and electrostatic forces. Gravitation is ignored, since the filter may have any orientation with respect to gravity. The gas velocity vector at each domain cell can be calculated by any of the above-described methods. With the Lagrangian method, the calculation of the flow field is accomplished before particle tracking is attempted, and the description of the flow field must be stored in computer memory, available to the particle-tracking computation.

The Eulerian approach treats particles as a second gas phase. The behavior of this second phase is calculated by the same method used for the carrier gas flow calculation, where possible. The incorporation of Brownian motion and electrostatic forces into the motion of gas packets would appear to be very artificial in concept, but these effects can be treated simply treated as added forces, spatially determined in the case of electrostatic forces, random in the case of Brownian motion. Studies of particle capture using other than Navier-Stokes equation with the finite-volume flow solution include Filippova and Hänel (1998), and Przekop, Moskal, and Gradon (2002), which use LB solutions for both flow and particle capture.

A hybrid approach for tracking particles divides the computational domain into zones where chosen methods are considered reliable. In our case, this would mean that for reliable results, the Eulerian approach could be used close to any fiber with *Kn* values >0.5. Elsewhere, the Lagrangian approach should be satisfactory. The definition of "close" becomes a variable in the solution, needing some experimentation comparing calculated results to experimental measurement to obtain the best value.

GAS AND MEDIA PROPERTIES

Methods for calculating these quantities and sources of needed coefficients are discussed in Part I. Table 2 lists values for a group of gases and operating conditions that are likely prospects for air filtration simulations or simulation verifications. Katz et al (2011) show how mixture properties are estimated.

The ranges of media properties and their measurement methods discussed in Part I are equally applicable to the methods described here. Special attention needs to be paid to the

properties of fibers and particles with nanometer characteristic dimensions, to determine when a fiber *Kn* is greater than 0.01.

SIMULATION OF FILTER MEDIA GEOMETRY IN FLOW DOMAINS

General requirements for media geometry descriptions are discussed in Part I. The choice of a computational grid (mesh) is sometimes more restricted than for the finite-volume method. Lattice-Boltzmann and DSMC procedures may use polygon cells for 2D and polyhedral cells for 3D, but the "unstructured" grids often used with finite-volume analyses are not permitted. The Lattice-Boltzmann method can interpolate values along curved boundaries, as shown in Figure 2 for the square cell case. Computational domains can also be divided into zones, each with different dimensioned but uniform cells, to allow more detail near boundaries or for other purposes.

MULTI-FIBER AIR FILTER MEDIA SIMULATIONS BEYOND THE NAVIER-STOKES EQUATION

Table 3 gives summaries of some air filter media simulation studies using equations and methods other than the Navier-Stokes/finite volume combination. We have limited the selections to simulations involving multiple fibers. Studies of the behavior of single fibers in essentially infinite domains can provide useful insights into particle capture and particle build-up on fibers, but ultimately we need to predict the performance of actual media, where the flow around each fiber is affected by its neighbors. We have not included studies which are purely theoretical, and are not verified, either directly by the authors' measurements on media simulated, or by data from earlier work. In actual air filter media under conceivable operating conditions, fiber

Reynolds numbers will not be as great as 20; we have not included studies with higher Reynolds numbers. These restrictions greatly reduce the number of examples for each of the methods described above.

IMPORTANT FACTORS NOT GENERALLY ADDRESSED IN SIMULATIONS

Several factors which can influence air filter performance have been largely neglected in simulations for both continuum and non-continuum flow: fiber binder volume, particle bounce, adhesion and equilibrium charge. Study of neglected factors for non-continuum flow is especially needed, since the physics of factors like particle adhesion may be different for rarefied gas conditions, or for nanofibers and nanoparticles.

CONCLUSIONS

Simulations of fibrous filter media for low-pressure applications and simulations for media incorporating fibers with diameters < 100 nanometers are unlikely to succeed using the Navier-Stokes equation and finite-volume solutions. Solutions based on the Burnett, Super-Burnett and Grad Moment methods extend the range of reliable solutions to only slightly higher fiber Kn values. Molecular dynamics, Lattice-Boltzmann and Direct Simulation Monte Carlo calculation methods all appear practical for specific flow regimes. It is not certain that the Boundary Singularity and Boundary Element Methods shorten computation times or indeed are possible for filter media simulations, but these methods should be investigated. More realistic geometric models for fibrous media require inclusion of fiber binders when these are present. Some media compress significantly when air flows through them, thus changing the geometry of the medium. 3D models of media geometry obviously can be made to model media more realistically than 2D models, but the shorter computation times of 2D may allow more fruitful

study of complicated effects. The validity of any CFD code, including user-supplied code additions, must be demonstrated by comparing simulation predictions with measurements on real media.

The effects of particle bounce and adhesion, and the effect of the electrostatic charges on nanoparticles in otherwise neutral aerosol clouds are substantial. Many studies of all these effects exist in the literature of aerosol technology, but there is need to evaluate which are the most accurate expressions for them, and incorporate the effects into any CFD method used. The goal of filter media performance simulation is ultimately to improve the design of filter media and filter structures, and to allow rational choices of filters for specific applications. The accuracy of such simulations needs to be known, especially where economics affects choices.

NOMENCLATURE

t = time, s

k = Boltzmann const., 0.0016448 J/K

M = molecular weight, kg kgmol^{-1}

Kn = Knudsen number, dimensionless

r = radius, m

p = pressure, Pa

T = temperature, K

R = gas constant, 8.31447J/molK

f = function, dimensionless

$\mathbf{u}$, $\mathbf{v}$, $\mathbf{c}$ = vector velocities, m/s

u,v = component of vector

● = vector dot product operator

d = diameter, m

∇ = vector divergence operator

Greek Symbols

λ	=	molecular mean free path, m	ρ	=	density, kg/m^3
μ	=	absolute viscosity, Pa-s	Ω_λ	=	collision integral
σ	=	stress tensor	θ	=	angle, radians

Subscripts

p = particle   f = fiber

g = gas   in = incident

REFERENCES

Agarwal, R.K., K.Y. Yun, and R. Balakrishian. 2001. Beyond Navier-Stokes: Burnett equations for flows in the continuum-transition regime. Physics of Fluids 13: 3061-3085. [Erratum: Physics of Fluids 14: 1818]

Allen, M.P. 2004. Introduction to molecular dynamics simulation. John von Neumann Institute für Computing Series 23: 1-28.

Baker, L.L. and N.G. Hadjiconstantinou. 2005. Variance reduction for Monte Carlo solutions to the Boltzmann equation. Physics of Fluids 17: 051703.

Bird, G.A. 1994. Molecular Gasdynamics and Direct Simulation of Gas Flows. Oxford, UK: Oxford University Press.

Bird, B.R., W.E. Stewart, and E. N. Lightfoot. 2002. Transport Phenomena 2nd Ed. Hoboken, NJ USA: Wiley.

Bobylev, A.V. 2006. Instabilities in the Chapman-Enskog expansion and hyperbolic Burnett equations. J. Statist. Phys. 124: 371-399.

Cercignani, C. 2000. Rarefied Gasdynamics: From Basic Concepts to Actual Calculations. Cambridge, UK, Cambridge University Press.

Chapman, S., and T.G. Cowling. 1970. The Mathematical Theory of Non-Uniform Gases, 3rd Ed., Cambridge, UK, Cambridge University Press.

Chen, S.Y., G.D. Doolen, and K.G. Eggert. 1994. Lattice-Boltzmann fluid dynamics: A versatile tool for multiphase and other complicated flows. Los Alamos Science 22: 98-111.

Comacho, R.G.R., and J.R. Barbosa. The boundary element method applied to incompressible viscous fluid flow. 2005. J. Brazilian Soc. Mech. Sci. Eng. 27: 456-462.

Filippova, O. and D. Hänel. 1996. Numerical simulation of particle deposition in filters. J. Aerosol Sci. 27: S627-S628.

Filippova, O. and D. Hänel. 1997. Lattice-Boltzmann simulation of gas-particle flow in filters. Computers and Fluids 26: 697-712.

Gad-el-Hak, M., The fluid mechanics of microdevices- The Freeman Scholar Lecture. 1999. ASME J. Fluids Eng. 121: 5-33.

Grad, H. 1949. On the kinetic theory of rarefied gases. Communications on Pure and Applied Math. 2: 331-407.

Hadjiconstantinou, N.G. 2006. The limits of Navier-Stokes theory and kinetic extensions for describing small-scale gaseous hydrodynamics. Physics of Fluids 18: 111301.

Hosseini, S. A. and H. V. Tafreshi. 2010. Modeling permeability of 3-D nanofiber media in slip flow regime. Chem. Eng. Science 65: 2249-2254.

Jennings, S.G. 1988. The mean free path in air. J. of Aerosol Sci. 19: 159-166.

Karniadakis, G., A. Beskok, and N. Aluru. 2005. Microflows and Nanoflows. New York: Springer.

Katz, I., G. Caillebotte, A.R. Martin, and P. Arpentinier, 2011. Property values estimation for inhaled therapeutic binary gas mixtures. Medical Gas Research 1: 28-40.

Kaye, G.W.C., T.H. Laby, J.C. Noyes, G.F. Phillips, O. Jones, and J. Asher. 1995. Tables of Physical and Chemical Constants, 16th Ed. London: Pearson Longman.

Luo, L.-S., M. Krafczyk, and W. Shyy, 2010. Lattice Boltzmann Method for Computational Fluid Dynamics.   Chap. 56 in Encyclopedia of Aerospace Engineering Vol. 1, Hoboken, New Jersey USA: Wiley.

Macrossan, M.N. 2006. Introduction to Direct Simulation Methods for Rarefied Flow. http://espace.library.uq.edu.au/eserve/UQ:8481/mnm_dsmc_course.pdf

Mazé, B., H.V. Tafreshi, Q. Wang, B. Pourdeyhimi. 2007. A simulation of unsteady-state filtration via nanofiber media at reduced operating pressures. J. Aerosol Sci. 38: 550-571.

McNenly, M.J., M.A. Gallis, and I.D. Boyd. 2005. Empirical slip and viscosity model performance for microscale   gas flow. Int. J. Numer. Meth. Fluids 49: 1169-1191.

Mei, R.W., W. Shyy, D.Z. Yu, and L.-S. Luo. 2002. Lattice Boltzmann method for 3-D flows with curved boundary. NASA/CR 2002-211657, ICASE Report No. 2002-17.

Muhammad, G., N. Shah, and M. Mushtaq, 2009. Merits and demerits of boundary element method for incompressible fluid flow problems. J. American Science 5: 57-61.

NIST. 2012 NIST SRD 134: Database of the Thermophysical Properties of Gases Used in the Semiconductor Industry. www.nist.gov/pml/div685/grp02/srd_134gasesindex.cfm.

NOAA/NASA/USAF, 1976. U.S. Standard Atmosphere. Washington: U.S. Government Printing Office (downloadable from Wikipedia)

O'Connell, S.T, and P.A. Thompson (1995) Molecular dynamics- continuum hybrid computations: a tool for studying complex flows. Physics Rev. E 52: R5792-R5795

Poling, B.E., J.M. Prausnitz and J.P. O'Connell. 2002. The Properties of Gases and Liquids 5th Ed. New York: McGraw-Hill.

Przekop, R., A. Moskal, and M.A. Gradon. 2002. Lattice-Boltzmann approach for description of the structure of deposited particulate matter in fibrous filters. J. Aerosol Science 34: 133-147.

Radtke, G.A., N.G. Hadjiconstantinou, and A.J. Wagner. 2011. Low-noise Monte Carlo simulation of the variable hard sphere gas. Physics of Fluids 23: 030606.

Raju, G.G., 2005. Gaseous Electronics: Theory and Practice. Boca Raton FL USA: CRC Press.

Rebaï, M., F. Drolet, D. Vidal, I. Vadeiko, and F. Bertrand, 2010. A lattice Boltzmann approach for predicting the capture efficiency of random fibrous media. Asia-Pacific J. Chem. Eng. 6: 29-37.

Reid, R.C., J.M. Prausnitz and B.E. Poling. 1987. The Properties of Gases and Liquids 4th Ed. New York: McGraw-Hill.

Sambaer, W., M. Zatloukal, and D. Kimmer, 2011. 3D Modeling of filtration process via polyurethane nanofiber based nonwoven fibers prepared by electrospinning process. Chem. Eng. Science 66: 613-626.

Sambaer, W., M. Zatloukal, and D. Kimmer, 2012. Air filtration modeling through polymeric nanofiber based filters. Proc. 11th World Filtration Cong. Session 002

Söderholm, L.H. 2007. Stabilizing the Burnett fluid dynamics equations. Proc. In Applied Math. And Mech. 7: 1141103-1141104.

Struchtrup, H. 2005. Failures of the Burnett and super-Burnett equations in steady state processes. Continuum Mech. Thermodynamics 17:43-50.

Struchtrup, H. and P. Taheri. 2011. Macroscopic transport models for rarefied gas flows: a brief review. IMA J. Applied Mechanics 76: 672-697.

Succi, S. 2001. The Lattice-Boltzmann Equations for Fluid Dynamics and Beyond. Oxford, UK: Oxford University Press.

Succi, S., M. Sbragaglia, and S. Ubertini, 2010. Lattice-Boltzmann Method. www.scholarpedia.org/article/Lattice_Boltzmann_Method

Torrilhon, M., and H. Struchtrup. 2008. Boundary conditions for regularized 13-moment-equations for micro-   channel–flows.   J. Computational Physics 227: 1982-2011.

Wagner, A.J. 2008. A Practical Introduction to the Lattice-Boltzmann Method. http://www.ndsu.edu/fileadmin/physics.ndsu.edu/Wagner/LBbook.pdf

Wang, C.Y., 2002. Stokes flow through a grid of circular cylinders. Physics of Fluids 14: 3358-3360.

Wang, X.P., K. Kim, C. Lee and J.Y. Kim. 2008a. Prediction of air filter efficiency and pressure drop in air filtration media using a stochastic simulation. Fibers and Polymers 9: 34-38.

Wang, J., S.C. Kim, D.Y.H. Pui. 2008b. Investigation of the figure of merit for filters with a single nanofiber layer on a substrate. J. Aerosol Science 39: 323-334.

Warth, T., and M. Piesche. 2010. Generation of three-dimensional nonwoven structures for simulation of fluid flow and particle deposition. In Proc. 7th Int'l Conf. on Multiphase Flow.

Yun, K.Y., and R.K. Agarwal. 2002. Burnett simulations of flows in microgeometries. In Proc. 3rd Int'l. Fluid Mechanics *Meeting, AIAA 2002-2870*, AIAA New York.

Zhao, S. 2009. Development of the Boundary Singularity Method for Partial-Slip and

Transitional Molecular-Continuum Flow Regimes with Application to Filtration. PhD

Thesis, University of Akron, Akron OH USA.

Zhao, S. and A. Povitsky. 2009. Boundary singularity method for partial slip flows. *Intl. J.*

Numerical Methods in Fluids 61: 255-274.

PART II –TABLE 1

Table 1. Flow Regimes, Knudsen Number Bounds, and Computation Methods

Knudsen Number Range	Flow Regime	Governing Equations and Computation Method	Code
Kn approaches 0	Continuum Flow, no molecular diffusion (zero viscosity)	Euler Equations	A
$Kn < 0.001$	Continuum Flow, molecular diffusion (viscous gas)	Navier-Stokes Equations without slip	B
$0.001 < Kn < 0.01$	Continuum-Transition Flow	Navier-Stokes Equations with partial slip	C
$0.001 < Kn < 0.1$	Continuum-Transition Flow	Burnett Equations with partial slip	D
$0.1 < Kn < 1.0$	Transition Flow	Burnett Equations With partial slip	E

0.1 < *Kn* < 1.0	Transition Flow	Grad Moment Equations	F
0.1 < *Kn* < 1.0	Transition Flow	DSMC	G
0.1 < *Kn* < 1.0	Transition Flow	Lattice-Boltzmann (LB)	H
Kn > 1.0	Free-Molecular Flow	Collisionless Boltzmann	J
Kn > 1.0	Free-Molecular Flow	Molecular Dynamics	K

Code B is often named the "no-slip" condition, codes C through H "partial-slip", and codes J and K "full-slip". BEM is applicable for codes A-C; BSM for codes B and C and DSMC and LB for codes A-H. MD is theoretically valid for all regimes.

PART II – TABLE 2

Table 2. Examples of Thermophysical Properties of Gases for Humid Air, Medical, and Semiconductor Process Gasses

Gas	Density ρ, kg/m^3	Viscosity μ, 10^{-6} Pa-s	Molecular Diameter d_m, nm	Mean Free Path λ, nm	Refs. (ρ,μ,d_m,λ)
Air, 0% R.H	1.204	18.19	0.366	65.43	1,1,1,1
Air, 50% R.H.	1.199	18.15	(mixture)	65.44	1,1,1,1
Air, 100% R.H.	1.194	18.13	(mixture)	65.48	1,1,1,1
Air, 0% R.H *	0.365	14.22	0.366	209.1	2,2,2,2

Oxygen	1.331	20.3	0.347	65.6	3,4,6,7
Nitrogen	1.182	17.6	0.380	60.9	3,4,6,7
Nitrous oxide	1.840	14.6	0.383	40.1	3,4,6,7
Carbon Dioxide	1.839	14.8	0.394	40.4	3,4,6,7
Ethylene Oxide	1.831	13.3	0.394	57.9	3,4,10,9
Argon	1.662	22.5	0.354	64.9	3,4,6,7
Helium	0.166	19.7	0.255	179.8	3,4,6,7
Hydrogen	0.0839	8.85	0.283	114.6	3,4,6,7
Silane	1.336	10.5	0.488	37.7	3,5,8,9
Nitrogen Trifluoride	2.935	16.9	0.394	58.3	3,4,10,9
Carbon Tetrafluoride	3.660	17.6	0.466	41.4	3,4,11 ,9

* This line gives properties of air at 11000 m, from

the US Standard Atmosphere (1976): pressure 22.700 kPa, temperature 216.77 K.

For all other gases in the table, pressure is 101.325 kPa, temperature 293.15 K.

References:

1. Jennings (1988)

2. NOAA/NASA/USAF (1976)

3. $\rho = ([\text{molecular weight}] /22.414) (273.15/293.15)$

4. $\mu = \mu^{\#}(293.15/300.00)^{1/2}$; $\mu^{\#}$ is the value for 300K from NIST SRD 134 (2012)

5. $\mu = \mu^{\#}(293.15/273.15)^{1/2}$; $\mu^{\#}$ is the value for 273.15K from the Air Liquide website

6. $d_m = d_m (293.15/273.15)$; d_m from Appendix E-1 of Bird et al (2002)

7. $\lambda = \lambda^{\#} (293.15/273.15)$; $\lambda^{\#}$ from Kaye et al (1995) [available as www.kayelaby.npl.co.uk]

ACCEPTED MANUSCRIPT

8. Raju (2005) p.293

9. $\lambda = \dfrac{m}{\pi\rho d_m{}^2 \sqrt{2}}$ where m is the mass of a molecule of the gas; $m = \dfrac{(molecular\,weight)}{1000 x 6.022142 x 10^{23}}$, kg;

Whence $\lambda = 3.73753 x 10^{-28}\,\dfrac{M}{\rho d_m^2}$, with both λ and d_m in meters.

10. Solve for d_m using $\mu = C_2\,\dfrac{\sqrt{MT}}{d_m^2 \Omega}$, with $C_2 = 2.6698$ x 10^{-5} and Ω as described in Bird et al (2002).

11. Reid et al (1987) Appendix B; Poling et al. (2002)

PART II – TABLE 3

Table 3. Some Simulations of Filtration by Fibrous Air Filter Media Not Using the Navier-Stokes / Finite Volume Method

Ref.	Media Form	Regime Code	CFD Method	Validation Method	Particle Diam.	Tracking Method	Results Given
1	3D/ Reg (3 fibers)	A	LB-BGK, no-slip	Cdata	UPD	Lagrange	Eff, PD
2	3D/UFD/RandL	~J	Modified MD	Cdata	Range	Lagrange	Eff. PD
3	2D/UFD/RegL	~E	NS/fvm	Cdata	Range	Lagrange/ Diffusion	Eff, PD
4	2D/UFD/RegL	~E	NS/fvm	Cdata	Range	Lagrange/	Eff.

			+slip BC			diffusion	PD
5	2D/UFD/RegL	A-~E	BSM/LB	Cdata, Cregr	none	none	PD
6	3D/UFD/RandL	~D	LB	Cdata	Range	Lagrange/ Brownian	Eff. PD
7	3D/UFD RegL/RandL	A	LB	Cdata	none	none	PD

UFD: uniform fiber diameter   3D: 3-Dimensional   2D: 2-Dimensional

RegL: fibers in a regular array   UPD: uniform particle diameter

RanL: fibers located randomly   Range: Range of particle diameters

   Eff: Efficiency   PD: pressure drop

Cdata: Compared to data   Creg: Compared to earlier data regressions

  fvm: finite volume method   MD: Molecular Dynamics method

  NS: Navier-Stokes equation   LB: Lattice-Boltzmann method

 BSM: Boundary Singularity Method   DSMC: Direct-simulation Monte Carlo

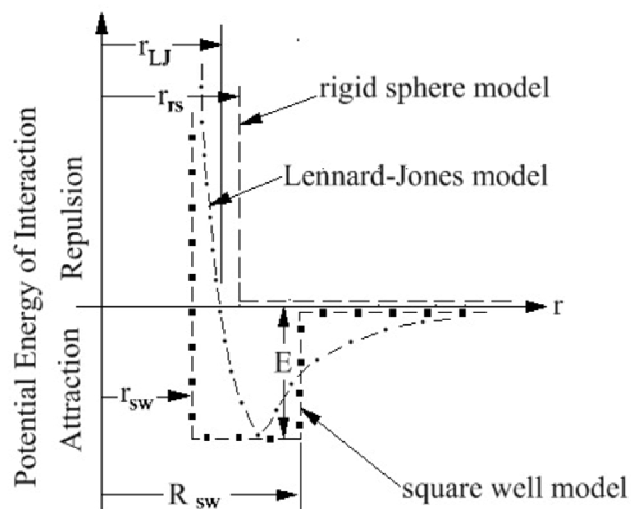 BGK: Bhatnagar-Gross-Krook   BC: Boundary conditions

References: 1: Filippova & Hänel (1997)   2: Mazé et al (2008)   3: Wang et al (2008a)

4: Wang et al (2009b)   5: Zhao (2009)   6: Rebaï et al (2010)   7: Warth and Piesche (2010)

PART II FIGURE CAPTIONS:

Figure 1. Approximations to the Potential Energy of Interaction Φ(*r*)

r = distance between centers of colliding molecules

r_{LJ} = collision radius = "molecular radius"
    (Attraction = Repulsion = 0)

r_{rs} = molecular radius, rigid sphere model

r_{sw} = inner well radius, square well model

R_{sw} = outer well radius, square well model

E = Characteristic energy of interaction

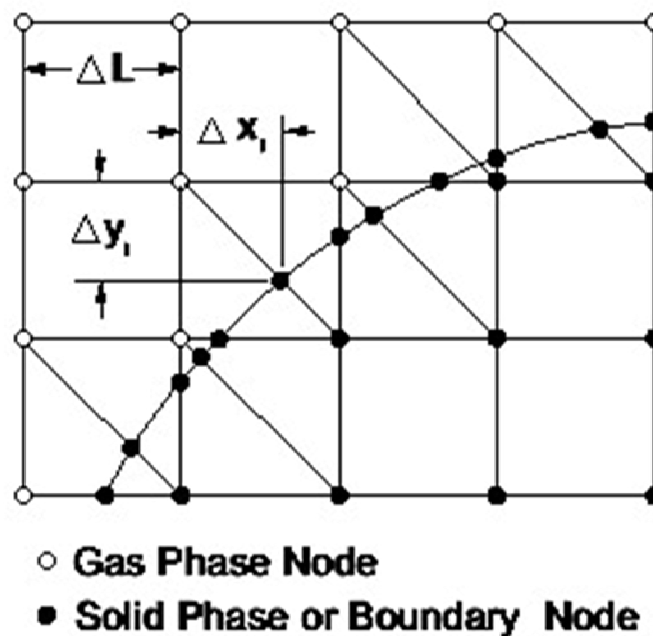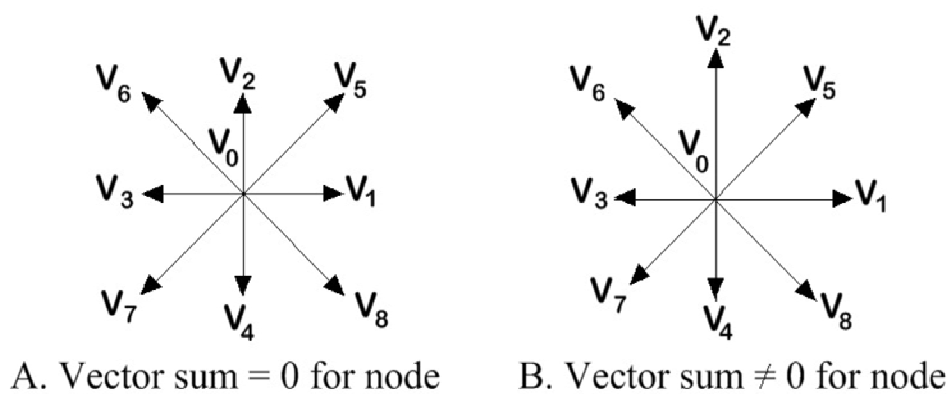**Figure 2. Lattice-Boltzmann Method: Lattice Geometry and Interpolations for a Curved Boundary**

Figure 3. Lattice-Boltzmann Vector Diagrams for a Single Node in Velocity Space

A. Vector sum = 0 for node   B. Vector sum ≠ 0 for node

Figure 4. Domain Model for Hybrid Finite Element/Molecular Dynamics Method (after O'Connell and Thompson (1995))

Continuum Zone →

Overlap Zone →

MD Zone →

A

C

B

V_B →

ACCEPTED MANUSCRIPT